An Endogenous Carbon-Sensing Pathway Triggers Increased Auxin Flux and Hypocotyl Elongation[1][C][W][OA]

Jodi L. Stewart Lilley[2], Christopher W. Gee[2], Ilkka Sairanen, Karin Ljung, and Jennifer L. Nemhauser*

Department of Biology, University of Washington, Seattle, Washington 98195 (J.L.S.L., C.W.G., J.L.N.); and Department of Forest Genetics and Plant Physiology, Umeå Plant Science Centre, Swedish University of Agricultural Sciences, SE–901 83 Umea, Sweden (I.S., K.L.)

The local environment has a substantial impact on early seedling development. Applying excess carbon in the form of sucrose is known to alter both the timing and duration of seedling growth. Here, we show that sucrose changes growth patterns by increasing auxin levels and rootward auxin transport in Arabidopsis (*Arabidopsis thaliana*). Sucrose likely interacts with an endogenous carbon-sensing pathway via the PHYTOCHROME-INTERACTING FACTOR (PIF) family of transcription factors, as plants grown in elevated carbon dioxide showed the same *PIF*-dependent growth promotion. Overexpression of *PIF5* was sufficient to suppress photosynthetic rate, enhance response to elevated carbon dioxide, and prolong seedling survival in nitrogen-limiting conditions. Thus, PIF transcription factors integrate growth with metabolic demands and thereby facilitate functional equilibrium during photomorphogenesis.

Nutrient and energy availability are key factors controlling growth in all organisms. This is particularly true of sessile plants, which use growth patterns to optimally exploit their local environment. "Functional equilibrium" describes the balancing act whereby plants modify the allocation of biomass to match resource availability and utilization across diverse environments (Poorter et al., 2012). Even in suboptimal light conditions, seedlings will undergo photomorphogenesis, unfurling their embryonic leaves (cotyledons) and decelerating growth in the embryonic stem (hypocotyl), to develop their photosynthetic capacity before seed reserves are exhausted. Seed reserves also contain nutrients required to support photomorphogenesis, but the developing root must quickly take over the task of nutrient acquisition. Photosynthetic rates in aboveground tissues shape the extent and pattern of growth in belowground organs, although how this growth is coordinated is largely unknown. The hypocotyl is a likely path for such signals, as it acts as a physical bridge between the carbon-fixing leaves and nutrient-acquiring roots, and the extent of hypocotyl elongation has long been used as a proxy for the strength of the light cue.

In addition to external environmental cues like light, hypocotyl growth is regulated by an endogenous timing mechanism (Nozue and Maloof, 2006). Circadian bursts of hypocotyl elongation occur even when plants are exposed to constant light, although light intensity can strongly influence growth rate within these windows. A model has recently been proposed to explain how dual control by light and the circadian clock produces peaks and troughs in hypocotyl growth rates. Both cues converge on the PHYTOCHROME-INTERACTING FACTOR (PIF) family of transcription factors, with clock regulation of *PIF* transcription and light regulation of PIF protein stability (Nozue et al., 2007). The result is a crepuscular pattern where seedling growth can occur at dawn and/or dusk. The relative proportion of growth at each twilight depends on the intensity of light, whether there are light/dark cycles, and the presence of supplemental Suc in the medium (Dowson-Day and Millar, 1999; Nozue et al., 2007; Stewart et al., 2011). The effect of Suc on hypocotyl growth patterns, as with light, is through the modulation of PIF protein abundance. While light promotes PIF protein turnover, Suc increases PIF abundance (Stewart et al., 2011).

Originally identified by their ability to directly bind with phytochrome photoreceptors, PIF transcription factors are now known to act as key growth regulators in response to a variety of environmental conditions

[1] This work was supported by the University of Washington Royalty Research Fund and the National Science Foundation (grant no. IOS–0919021), by the Swedish Governmental Agency for Innovation Systems and the Swedish Research Council, by the National Science Foundation Graduate Research Fellowship Program and the Seattle Chapter of the Achievement Rewards for College Scientists Foundation to J.L.S.L., and by a Summer Undergraduate Research Fellowship from the American Society of Plant Biology and a College of Arts and Sciences Undergraduate Research Award to C.W.G.

[2] These authors contributed equally to the article.

* Corresponding author; e-mail jn7@uw.edu.

The author responsible for distribution of materials integral to the findings presented in this article in accordance with the policy described in the Instructions for Authors (www.plantphysiol.org) is: Jennifer L. Nemhauser (jn7@uw.edu).

[C] Some figures in this article are displayed in color online but in black and white in the print edition.

[W] The online version of this article contains Web-only data.

[OA] Open Access articles can be viewed online without a subscription.

www.plantphysiol.org/cgi/doi/10.1104/pp.112.205575

(Leivar et al., 2009; Kumar et al., 2012; Li et al., 2012). Several recent studies have connected PIF-mediated growth control to the hormone auxin (Franklin et al., 2011; Nozue et al., 2011; Li et al., 2012; Sun et al., 2012). *YUCCA8* and *TRYPTOPHAN AMINOTRANSFERASE OF ARABIDOPSIS1* (*TAA1*), encoding auxin biosynthetic enzymes, have been shown to be direct targets of PIF4 (Franklin et al., 2011; Sun et al., 2012). PIF7 has also been shown to directly bind to *YUCCA8* to increase stem growth in response to shade (Sun et al., 2012). Loss of function in PIF family members reduces auxin responsiveness (Nozue et al., 2011), and this relationship might partially explain circadian fluctuations in seedling sensitivity to exogenous auxin (Covington and Harmer, 2007).

In this study, we show that supplemental Suc stimulates an endogenous carbon-sensing pathway that regulates hypocotyl elongation through altered auxin levels and distribution in Arabidopsis (*Arabidopsis thaliana*). Previously, we have shown that Suc is required for sustained and rhythmic hypocotyl elongation (Stewart et al., 2011). Here, we found that exogenous auxin could mimic the spatial and temporal growth effects of Suc. Seedlings grown with supplemental Suc had higher levels of free auxin and increased rootward auxin transport. As Suc-driven changes in both auxin levels and seedling growth were *PIF* dependent, we propose that PIF proteins integrate information about fixed carbon availability with other photomorphogenetic cues to shape seedling morphology. In support of this model, exposure to elevated levels of CO_2 stimulated hypocotyl growth in a *PIF*-dependent manner. Suc was also found to suppress seedling photosynthetic rates and increase nitrogen demand, physiological responses predicted for high-fixed-carbon conditions. Consistent with the *PIF* family acting as a relay point in carbon sensing, overexpression of *PIF5* sensitized plants to elevated CO_2, strongly reduced photosynthetic rates, and promoted prolonged seedling survival in nitrogen starvation conditions.

RESULTS

Suc Increases Auxin Levels

The hypocotyl elongates until the cotyledons are fully opened, a period lasting approximately 4 d post germination (dpg) in short-day conditions (Stewart et al., 2011). Brassinosteroids, auxin, and gibberellins are well-studied promoters of seedling growth (Nozue and Maloof, 2006). Treatment with any of these hormones increased hypocotyl growth rates prior to day 4 (Fig. 1A). In contrast, only seedlings grown in the presence of the synthetic auxin picloram or the natural auxin indole-3-acetic acid (IAA) showed substantial growth into day 5 (Fig. 1, A–C). These auxin-induced effects on growth dynamics were strikingly similar to those caused by supplementation with Suc (Stewart et al., 2011). In addition, auxin and Suc treatments had a similar effect on a reporter marking the hypocotyl elongation zone (*PHYTOCHROME KINASE SUBSTRATE4* [*PKS4*::GUS]; Schepens et al., 2008). While reporter expression was greatly reduced after 4 dpg in untreated seedlings, treatment with either Suc or auxin led to strong staining through day 5 (Fig. 1C), consistent with continued growth.

The similar pattern of growth between the two treatments led to the hypothesis that Suc might be directly acting on the auxin pathway. Suc supplementation reduced the threshold for maximum auxin-induced growth by 5-fold (Fig. 1D). In addition, Suc caused a sharp reduction in the levels of the DII-VENUS reporter (Fig. 1E), which is rapidly turned over in the presence of auxin (Brunoud et al., 2012). Both of these results are consistent with Suc leading to higher endogenous levels of auxin. Expression of a number of early auxin response genes, including *INDOLE-3-ACETIC ACID17* (*IAA17*), *IAA19*, *IAA29*, and *SMALL AUXIN UP-REGULATED15* (*SAUR15*), was modestly upregulated in the presence of Suc, especially in isolated shoots (Fig. 1F; Supplemental Table S1). A nonmetabolizable Suc analog was previously shown to induce auxin-responsive genes (Gonzali et al., 2005), suggesting that Suc may be acting as a direct signaling molecule.

Suc was found to significantly increase the amount of IAA per mg fresh weight in whole seedlings (Fig. 1G). Suc promotion of IAA levels was most clearly observed in dissected hypocotyls or roots (Fig. 1G). This finding is consistent with recent feeding experiments with heavy-labeled auxin precursors that indicate that sugars can induce auxin biosynthesis in both shoot and root tissue (I. Sairanen and K. Ljung, unpublished data). The effect of Suc on auxin levels may be through altered expression of auxin biosynthetic genes. Expression of *YUCCA8* was induced by Suc in the shoot (Fig. 1F), but expression of *TAA1* was unchanged with Suc treatment (Fig. 1F).

Suc Promotes Rootward Auxin Transport

Suc was able to promote primary root elongation (Fig. 2A), as might be expected given the higher levels of auxin in such conditions (Fig. 1G). Increasing endogenous auxin production in the *yucca-D* mutant could partially phenocopy this response and caused a reduced sensitivity to Suc (Fig. 2A). As auxin is synthesized at a high rate in the shoot apex and in young, developing leaves (Ljung et al., 2001), we hypothesized that Suc promotion of IAA levels in hypocotyls and roots might reflect an increase in rootward auxin transport. Inhibiting auxin transport with 1-*N*-naphthylphthalamic acid (NPA) completely blocked Suc-induced growth (Fig. 2B). Seedlings mutated at the *MORE AXILLARY BRANCHES2* locus (*max2* mutants), which have a constitutively increased rate of auxin transport (Bennett et al., 2006), were taller than wild-type seedlings and had a 70% reduction in Suc response (Fig. 2C). Moreover, wild-type seedlings grown on Suc showed a nearly identical hypersensitivity to NPA treatments

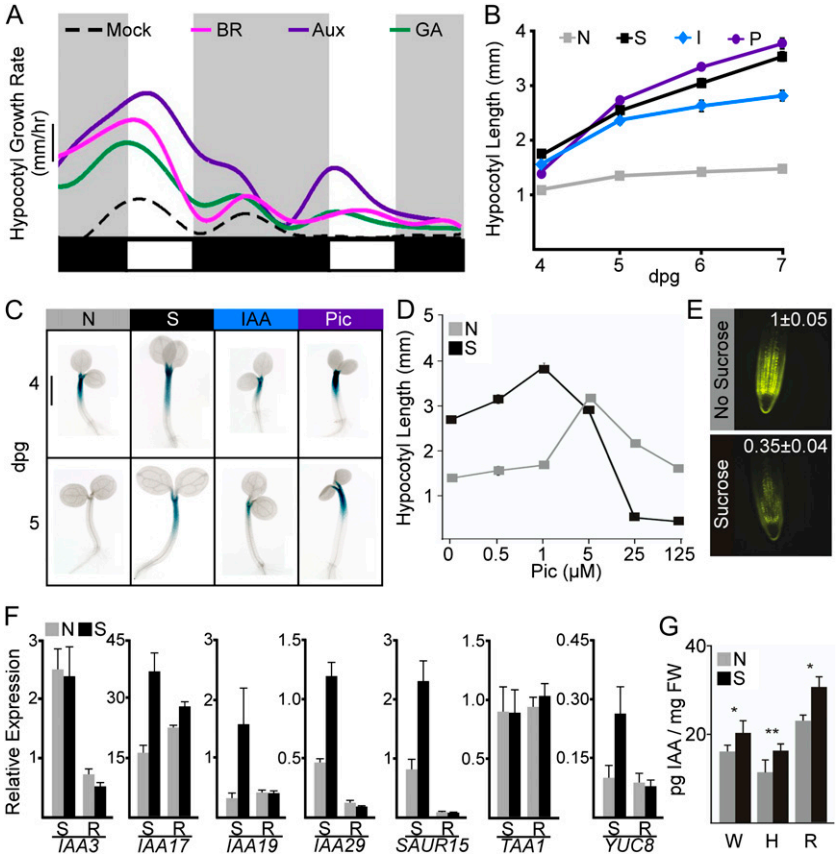

Figure 1. Suc stimulates the auxin pathway. A, Hypocotyl elongation rates of seedlings exposed to the growth-promoting hormones brassinosteroid (BR), auxin (Aux), and gibberellin (GA). Smoothed average growth rates from three independent experiments (representing an average of 15–20 seedlings per experiment) are shown. The dashed black line indicates growth rates on medium without hormone supplementation (mock). Light and dark phases are indicated in the bars below the graphs, beginning with midnight of the 3rd dpg. Bar = 0.05 mm h^{-1}. B, Suc (S), natural auxin (IAA [I]), and synthetic auxin (picloram [P]) prolonged hypocotyl elongation when compared with seedlings grown without any treatments (N). Error bars represent SE. Some error bars are within the boundaries of the markers. C, Seedlings carrying the PKS4::GUS reporter showed similar GUS expression in the elongating region of the hypocotyl for Suc- and auxin-treated seedlings. Bar = 1 mm. D, Seedlings grown on Suc showed an increased sensitivity to picloram (Pic). Error bars represent SE. Some error bars are within the boundaries of the markers. E, Root tips of plants grown on Suc had a reduction in fluorescence of the auxin-degradable DII-VENUS reporter. Representative images are shown with fluorescence quantification values normalized to the no-Suc mean ± SE for 25 seedlings. F, Quantitative reverse transcription-PCR shows that Suc increases the expression of several auxin-induced genes. Suc effects on gene expression are much stronger in shoots (S) compared with roots (R). Error bars represent SE. G, Suc (S) increased endogenous auxin levels when compared with plants grown without added Suc (N) in whole seedlings (W), hypocotyls (H), and roots (R). Error bars represent SE. Asterisks indicate significant differences between Suc and no-Suc treatments for both genotypes (*$P < 0.05$, **$P < 0.01$) using Student's *t* test and a Hommel multiple comparison correction. FW, Fresh weight. [See online article for color version of this figure.]

as untreated *max2* mutants (Fig. 2D). We analyzed the expression of three genes encoding PIN-FORMED (PIN) auxin transporters strongly associated with auxin delivery to the root tip (Blilou et al., 2005). Of these, Suc induced the expression of *PIN7* (Fig. 2E). Expression of *IAA3*, encoding a negative regulator of *PIN7* (Dello Ioio et al., 2008), was repressed by Suc in shoots but not in roots (Fig. 1F). Since the effect of Suc on *PIN* expression is modest, Suc may affect the posttranslational regulation of PIN activity (Grunewald and Friml, 2010).

To more directly test for a Suc effect on auxin movement, we assayed the response dynamics of auxin reporters to local auxin application. We applied IAA microdrops to a single cotyledon of plants expressing the synthetic auxin response reporter DR5::GUS (Fig. 2F). In seedlings grown without Suc, the reporter was induced throughout the treated cotyledon within a few hours. In the same time frame, Suc-grown seedlings showed a dramatic extension of reporter expression down the entire length of the hypocotyl (Fig. 2D). Results were similar with a natural auxin-responsive reporter (pS15-5E::GUS; Walcher and Nemhauser, 2012; Supplemental Fig. S1). Exposing seedlings to double the intensity of light produced a hybrid phenotype

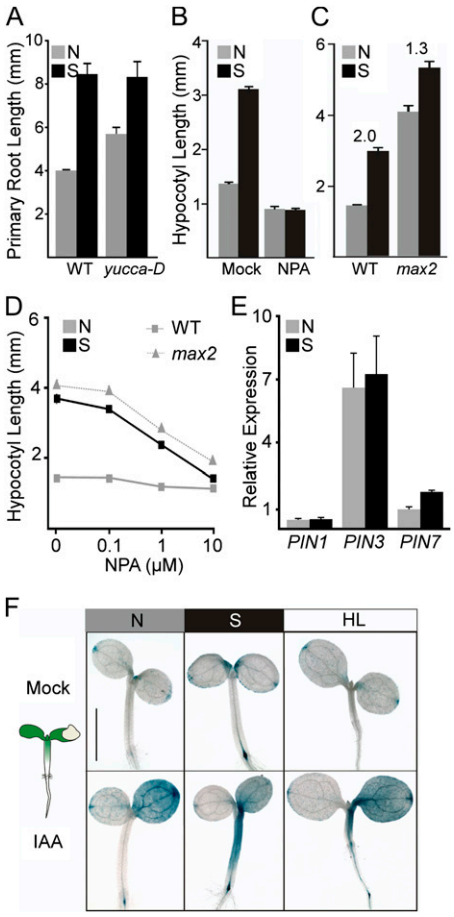

Figure 2. Suc promotes rootward auxin transport. A, Suc increased primary root length. Higher endogenous auxin levels in the *yucca-D* mutants led to longer primary roots and a reduced response to Suc. Error bars represent SE. B, Blocking auxin transport with 50 μM NPA eliminated Suc-induced hypocotyl elongation. Error bars represent SE. C, Mutants with increased auxin transport (*max2*) were less sensitive to Suc. Ratios of hypocotyl length in Suc (S) versus non-Suc (N) conditions are indicated. Error bars represent SE. D, Suc addition to wild-type (WT) seedlings (squares) increased sensitivity to the auxin transport inhibitor NPA, making them resemble *max2* mutants (triangles) grown without Suc. Error bars represent SE. Some error bars are within the boundaries of the markers. E, Suc induces expression of the gene encoding auxin efflux carrier PIN7 but has no measurable effects on genes encoding PIN1 or PIN3. Error bars represent SE. F, Suc increases rootward auxin transport, as measured by the increased distance of auxin reporter staining from the site of local auxin application (depicted in the schematic at left). Exposing seedlings to increased light intensity (HL) was sufficient to increase staining distance. Bar = 1 mm for the no-Suc panel and 1.3 mm for all others. [See online article for color version of this figure.]

(Fig. 2F). Light likely increases endogenous Suc production through increased photosynthesis (Poorter et al., 2012), yet it also inhibits stem growth through the degradation of *PIF* proteins (Leivar and Quail, 2011). Similar to Suc treatment, seedlings grown in higher light showed an apparent increase in rootward auxin transport; yet, unlike Suc treatment, they exhibited reduced hypocotyl elongation (Fig. 2F). This complex phenotype highlights potential organ-specific differences in the composition and function of photomorphogenetic pathways.

Suc Effects on the Auxin Pathway Are Both *PIF* Dependent and Independent

As Suc promotion of sustained seedling growth requires *PIF* genes (Stewart et al., 2011), we wondered whether the same would be true for auxin. We found that auxin increased late-phase seedling growth rates by approximately 4-fold and that this growth promotion was substantially reduced in *pifQ* mutants lacking functional *PIF1*, *PIF3*, *PIF4*, and *PIF5* (Fig. 3A). A reduced auxin sensitivity of *pifQ* mutants has been observed in previous studies (Nozue et al., 2011). This phenotype places the *PIF* genes downstream from the auxin signal; however, quantification of IAA levels in *pifQ* mutants found a substantial reduction in the effect of Suc (Fig. 3B). To further complicate the genetic model, *pifQ* mutants showed modestly higher concentrations of IAA than wild-type plants. The same trend was observed in the primary root; *pifQ* roots were longer than the wild type without supplementary Suc and showed a reduced Suc response (Supplemental Fig. S2). Auxin-induced gene expression is similarly complex in *pifQ* mutants supplemented with Suc. In shoots of wild-type plants, Suc induced the expression of *IAA17*, *IAA19*, and *IAA29* by 2.3-, 5-, and 2.6-fold, respectively (Fig. 1F; Supplemental Table S1). In *pifQ* mutants, the Suc response of these same genes was reduced to only 1.4-, 2-, and 2.1-fold, while the approximate 3-fold induction of *SAUR15* was similar to the wild-type response (Fig. 3C; Supplemental Table S1). Suc induced the expression of *YUCCA8* by 2.7-fold in wild-type shoots and by 5.4-fold in *pifQ* shoots (Figs. 1F and 3C; Supplemental Table S1). One possible explanation for these results is feedback regulation, whereby *PIF* genes effectively act both upstream and downstream of auxin, with differential responses in particular tissues or on particular promoters. In this way, the *PIF*-auxin pathway may resemble the nonlinear relationship between *PIFs* and the phytochrome photoreceptors (Leivar and Quail, 2011).

To further clarify the relationship between auxin and *PIF* genes, we tested the effects of auxin on *PIF* gene expression and levels of PIF5 protein. In these assays, we used the synthetic auxin picloram, as IAA inhibits seed germination and interferes with early seedling development. Recent transcriptome studies on isolated hypocotyls found that picloram and IAA effects were largely indistinguishable (Chapman et al., 2012). Similar to Suc, auxin produced only modest changes in *PIF* gene expression (Supplemental Fig. S3). We have previously shown that Suc dramatically increases the abundance of PIF5 in the dark and light (Stewart et al., 2011). However, unlike Suc, we could not detect any effect of auxin on PIF5 abundance (Fig. 3D). This suggests that the effect of Suc on PIF abundance is upstream of auxin biosynthesis and transport.

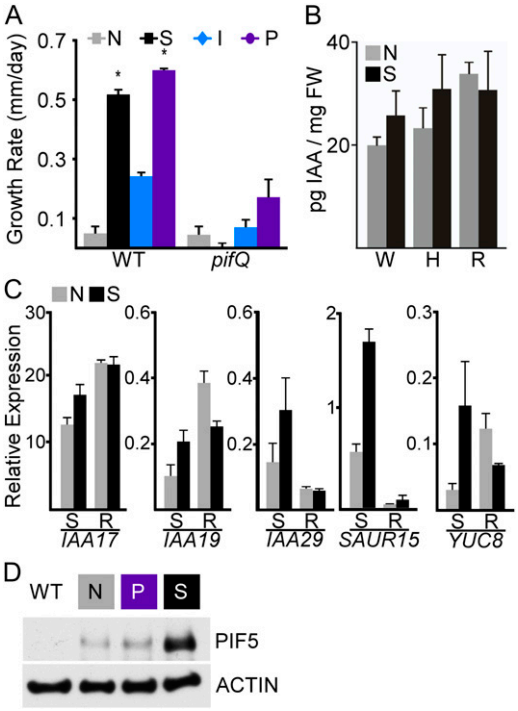

Figure 3. Suc effects on auxin require *PIF* genes. A, Growth promotion by auxin or Suc in wild-type seedlings (WT) was greatly diminished in *pifQ* mutants. Growth rates from day 5 are shown. Error bars represent SE. Asterisks indicate significantly different rates ($P < 0.05$) between the tested treatment and the no-Suc treatment for the wild type and *pifQ* using Student's *t* test and a Hommel multiple comparison correction. B, *pifQ* mutants show no significant effect of Suc on IAA levels in whole seedlings (W), hypocotyls (H), or roots (R). Error bars represent SE. FW, Fresh weight. C, Suc effects on some but not all auxin-responsive genes were diminished in *pifQ* mutants. R, Roots; S, shoots. Error bars represent SE. D, Suc caused a clear increase in PIF5 levels, while auxin (picloram [P]) had little effect. Wild-type or 35S::PIF5-HA seedlings were collected at dawn on day 5. Anti-HA antibodies were used to detect PIF5-HA proteins (top panel), and anti-actin antibodies were used as a loading control (bottom panel). [See online article for color version of this figure.]

Suc Triggers an Endogenous Carbon-Sensing Pathway

For a seedling germinating in natural settings, Suc would be supplied largely through photosynthesis. *PIF* genes have an established role in repressing photomorphogenesis and development of the photosynthetic apparatus in the dark (Moon et al., 2008; Toledo-Ortiz et al., 2010). To assess the effects of Suc on photosynthesis, we measured rates of carbon uptake in wild-type seedlings under a range of light conditions with and without supplemental Suc. Addition of Suc reduced rates of carbon uptake in our standard light conditions (60 μmol m^{-2} s^{-1}), resulting in a net negative rate of CO_2 assimilation (Fig. 4A, inset). Suc may act on photosynthesis through sugar-mediated feedback (Paul and Foyer, 2001), by a shift in biomass allocation that increases respiration rates, or by a combination of these and yet to be determined factors. *pifQ* mutants behaved essentially the same as wild-type plants in these experiments, suggesting that there is compensation for any increased expression of photosynthesis-related genes (Moon et al., 2008; Toledo-Ortiz et al., 2010). In contrast, plants overexpressing *PIF5* had dramatic reductions in assimilation rate at all light levels and a much-reduced light-saturated assimilation rate (Fig. 4A). This reduction in photosynthetic capacity likely reflects the limited expansion of the cotyledons in *PIF5ox* seedlings (Supplemental Fig. S4, A–C) as well as the antagonism between *PIFs* and the photomorphogenesis program. We also analyzed stomatal density as a possible cause of altered photosynthetic rates, but *PIF5ox* plants actually showed an increased number of stomata per cotyledon area when compared with the wild type or *pifQ* mutants (Supplemental Fig. S4D).

Another effect of supplemental Suc is an increase in the seedling's carbon-to-nitrogen ratio, a driving force in models of functional equilibrium. To test whether Suc was intersecting with an endogenous carbon-sensing pathway, we grew plants in approximately twice the concentration of atmospheric CO_2. Elevated CO_2 recapitulated the effects of Suc on seedling growth: seedlings grown in higher CO_2 were significantly taller than controls, and this effect required *PIF* genes (Fig. 4B). *pifQ* mutants were unable to respond to elevated CO_2, while *PIF5ox* seedlings showed a stronger response than the wild type (Fig. 4B). As an additional control, we measured the effects of elevated CO_2 on *max2* mutants, which are nearly as tall as *PIF5ox* seedlings in ambient CO_2. In contrast to *PIF5ox*, *max2* mutants showed a reduced response to elevated CO_2, indicating that increased rates of auxin transport alone are not sufficient to confer CO_2 hypersensitivity (Fig. 4B).

Excess carbon would be predicted to induce nitrogen assimilation pathways to balance carbon-to-nitrogen ratios. Suc addition caused a severe bleaching phenotype in plants germinated on nitrogen-deficient medium, suggesting that Suc led to a more rapid depletion of nutrients in seed reserves (Fig. 4C). *pifQ* mutants behaved similarly to wild-type plants, but *PIF5ox* plants were resistant to nitrogen limitation. This pattern may reflect the differential photosynthetic rates observed in these genotypes (Fig. 4A) and the resulting differences in nitrogen demands. In relatively nitrogen-rich standard medium, Suc treatments increased the expression of *NITRATE TRANSPORTER1.1* (*NRT1.1*), encoding a transporter of both nitrate and auxin (Krouk et al., 2010; Fig. 4D). Expression of this gene is associated with the acquisition of nitrogen (Forde, 2002). The root nitrogen assimilation response does not require *PIF* genes, as *pifQ* mutants showed similar patterns of gene expression as wild-type seedlings (Fig. 4D). Another consequence of adding Suc is increased osmotic stress; however, treatment with equimolar mannitol did not recapitulate Suc effects (Supplemental Fig. S5; Stewart et al., 2011).

DISCUSSION

In this study, we provide mechanistic links between several well-studied regulators of photomorphogenesis.

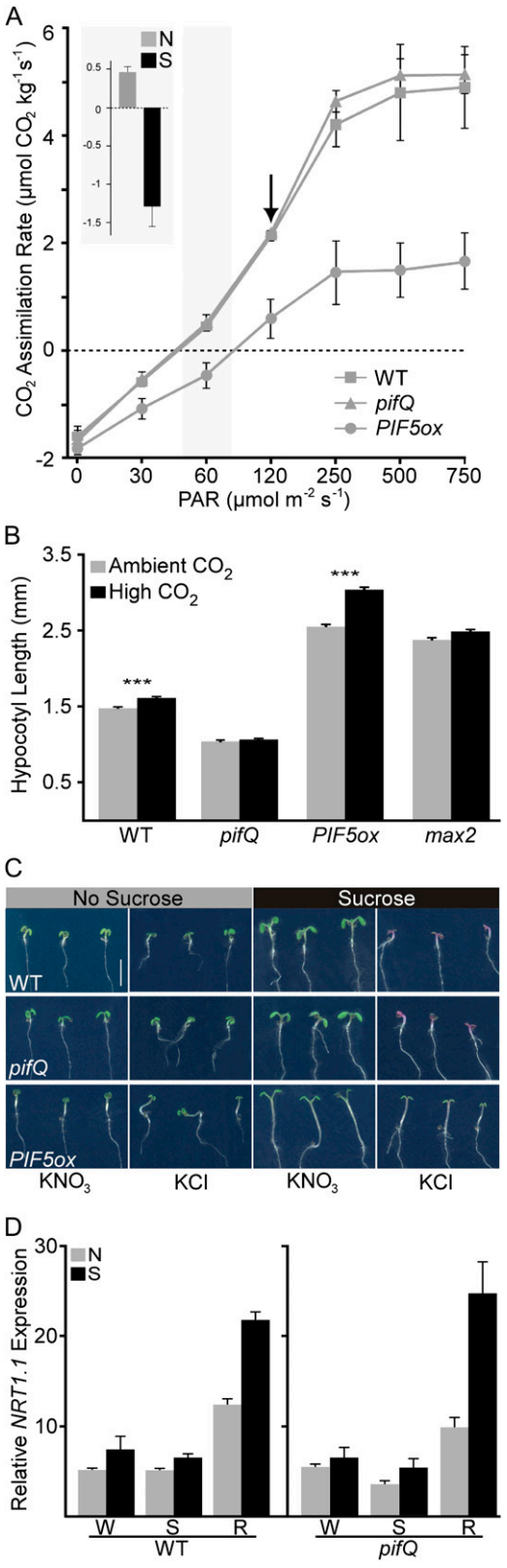

Figure 4. Suc stimulates an endogenous carbon-sensing pathway. A, CO_2 assimilation rates of wild-type (WT), *pifQ*, and *PIF5ox* seedlings were quantified over a range of light intensities (photosynthetically active radiation [PAR]). Overexpression of *PIF5* reduced net carbon uptake. CO_2 assimilation rates of wild-type seedlings on medium with and without Suc at the standard growth conditions of this study (60 μmol m^{-2} s^{-1}; gray shading) are shown in the inset. The black arrow indicates the photosynthetic rate under the conditions for the high-light experiment shown in Figure 2D. Error bars represent SE. B, Wild-type seedlings grown in elevated CO_2 (approximately 800 μL L^{-1}; black) showed a small but significant increase in height compared with seedlings grown in ambient CO_2 (approximately 400 μL L^{-1}; gray). This response was completely abolished in *pifQ* mutants. Overexpression of *PIF5* (*PIF5ox*) greatly enhanced the growth promotion effect of elevated CO_2. In *max2* mutants, where auxin transport is constitutively increased, response to increased CO_2 was reduced. Error bars represent SE for four independent experiments. Asterisks indicate significant differences between ambient and elevated CO_2 treatments for each genotype using an ANOVA with Tukey's pairwise comparisons (***$P < 0.001$). C, Suc supplementation led to bleaching in low-nitrogen conditions by 8 dpg. Seedlings were grown on low-nitrogen medium supplemented with either 0.5 mM KNO_3 or equimolar KCl. *PIF5ox* seedlings remained green in all medium conditions. Bar = 5 mm. D, Suc strongly induces the gene encoding NRT1.1, a nitrate-sensitive auxin transporter. The induction of *NRT1.1* can be detected in whole seedlings (W) but appears stronger in dissected roots (R) when compared with dissected shoots (S). This effect of Suc is not *PIF* dependent, as it is still detectable in *pifQ* mutants. Error bars represent SE. [See online article for color version of this figure.]

First, we found that supplemental Suc promoted hypocotyl elongation through altered auxin levels and distribution (Figs. 1 and 2). Second, we found that Suc likely activated an endogenous *PIF*-dependent carbon-sensing pathway (Figs. 3 and 4). Overexpression of *PIF5* was sufficient to alter whole-plant metabolism, decreasing both the rate of carbon assimilation and nitrogen demand (Fig. 4). It is already well established that PIF transcription factors are key regulators of growth and development in response to a variety of environmental conditions (Leivar et al., 2009; Kumar et al., 2012; Li et al., 2012). Our results suggest an expanded model where PIF proteins act as points of integration for metabolic cues during photomorphogenesis and daily growth cycles (Fig. 5).

Our previous work demonstrated that rhythmic seedling growth requires supplementation with excess carbon in the form of Suc and that Suc effects on growth are *PIF* dependent (Stewart et al., 2011). This study showed that auxin mimicked Suc supplementation and that auxin-stimulated hypocotyl elongation required *PIF* genes. Our findings add weight to those of several recent studies proposing a strong link between auxin and the *PIF* family (Franklin et al., 2011; Nozue et al., 2011; Li et al., 2012; Sun et al., 2012). However, our data also show that the relationship between *PIF* genes and auxin is complex. While *pifQ* mutants were largely insensitive to the growth-promoting effects of exogenous auxin (Fig. 3A) and did not show significant changes in endogenous IAA levels following Suc treatment (Fig. 3B), *pifQ* mutants did show overall higher levels of IAA (Fig. 3B). This result, in combination with differential effects of the loss of *PIF* function on Suc induction of auxin-stimulated genes (Fig. 3C), suggests that there may be *PIF*-dependent and *PIF*-independent

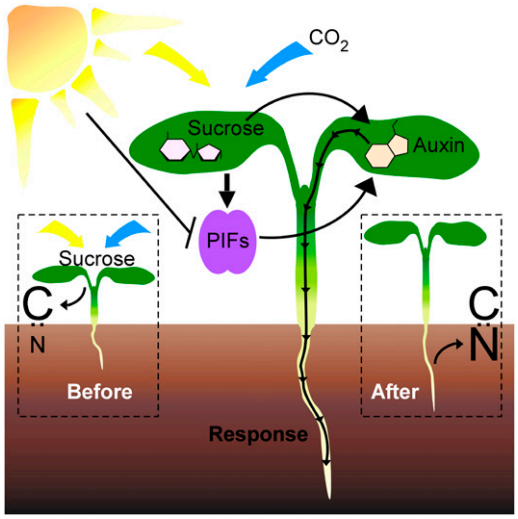

Figure 5. A model of a *PIF*- and auxin-mediated carbon-sensing pathway. Light (yellow arrow) and CO_2 (blue arrow) elevate endogenous Suc and thus carbon (C) levels (Before). Suc then stimulates both PIF-dependent and -independent auxin responses (Response), promoting hypocotyl and root elongation. These elongated roots acquire nitrogen (N) from the soil, and the carbon-nitrogen balance is restored (After). [See online article for color version of this figure.]

branches within the auxin biosynthetic and response pathways. In addition, PIFs have recently been shown to act as negative regulators of sugar-induced IAA biosynthesis in seedlings grown in liquid culture (I. Sairanen and K. Ljung, unpublished data). This suggests that even in the *PIF*-dependent branches of Suc-induced auxin response, the PIFs may be playing both positive and negative roles.

Rhythmic hypocotyl elongation observed with supplemental Suc may represent an amplified read-out of the endogenous daily rhythms of interorgan communication. In support of this, IAA biosynthetic rates are nearly twice the level at dusk than at dawn without sugar supplementation (I. Sairanen and K. Ljung, unpublished data). This is precisely the period when hypocotyl elongation rates are fastest in the absence of Suc (Stewart et al., 2011). Information regarding carbon availability in the leaves must be conveyed to the roots, and the hypocotyl is the physical connection between these organs. Rhythmic hypocotyl elongation may reflect the coordination of growth, with the availability of raw materials and energy tied to daily fluctuations in photosynthesis. The lack of Suc response in the *pifQ* mutants (Fig. 3, A and B) and the altered metabolism of *PIF5ox* plants (Fig. 4, A–C) support a model where the *PIF* family is at the center of this coordination (Fig. 5). By refining the timing and magnitude of hypocotyl elongation through modulating levels of PIF proteins, carbon availability can be easily incorporated into an expanded coincidence model of rhythmic growth (Nozue et al., 2007). Here, we have shown that Suc increases both auxin content and transport to the root (Figs. 1G and 2F). While blocking auxin transport prevents Suc-induced hypocotyl elongation (Fig. 2B), it is unclear if increased biosynthesis is also required for growth or if transport alone is sufficient. As levels of auxin strongly influence auxin transport rates (and perhaps vice versa), it is difficult to experimentally isolate effects on auxin biosynthesis from those on transport (Grunewald and Friml, 2010).

Our results suggest that, in addition to regulating hypocotyl elongation, auxin acts a shoot-to-root signal for nitrogen demand. Cytokinins have been identified as a systemic root-to-shoot signal of nitrogen supply (Kiba et al., 2011; Ruffel et al., 2011), but definitive identification of a complementary shoot-to-root signal has remained elusive. Auxin has been proposed as a candidate nitrogen-demand signal, as it is transported from the shoots to the roots and positively regulates lateral root development (Forde, 2002; Walch-Liu et al., 2006; Macgregor et al., 2008; Kiba et al., 2011; Ruffel et al., 2011). In addition, plants show increased root auxin levels in response to a drop in nitrogen availability (Walch-Liu et al., 2006). Here, we show that auxin levels increased in response to higher carbon levels and that this response was most striking in roots (Fig. 1G). Suc induction of the gene encoding the nitrate-sensitive auxin transporter NRT1.1 (Fig. 4D) strengthens the link between high carbon, increased auxin accumulation in the roots, and, ultimately, increased nitrogen uptake (Krouk et al., 2010; Kircher and Schopfer, 2012).

Functional equilibrium during photomorphogenesis relies on differential biomass allocation between three organ systems: cotyledons, hypocotyls, and roots. While the relative growth rate of cotyledons versus the hypocotyl is a key measure of light response, less attention has been paid to how root area affects metabolic homeostasis during the transition to photoautotrophy. A recent study reported that photosynthate from cotyledons is needed for substantial root growth, independent of the phytochrome and cryptochrome photoreceptors (Kircher and Schopfer, 2012). Previous studies have shown that application of Suc to shoots alone is sufficient for the promotion of lateral root outgrowth (Macgregor et al., 2008). The enhanced root growth and reduced sensitivity to Suc seen in the *yucca-D* mutants (Fig. 2F) suggest a model for combinatorial regulation of root patterning by both photosynthate and auxin. This is further supported by the correlation of high auxin levels, elongated primary root, and low Suc response observed in *pifQ* mutants (Fig. 3B; Supplemental Fig. S2).

Nutrient limitation is thought to partially explain why many plant species fail to sustain high growth rates in elevated CO_2 (Stitt and Krapp, 1999). The challenge of coordinating local metabolic conditions with growth across a multicellular organism is not unique to plants. In animals, the TOR pathway integrates nutrient and energy sensing with growth control (Hietakangas and Cohen, 2009). Intriguingly, recent transcriptional data suggest that sugar, auxin, and cytokinin all converge on the plant TOR pathway (Dobrenel et al., 2011). While many of the specific members of the animal TOR pathway do not have readily identifiable plant homologs,

further studies will be needed to judge the extent of functional conservation between animal and plant pathways. A mechanistic understanding of how metabolism shapes plant biomass allocation will be critical to predict and manage productivity across diverse environments, particularly in response to rising CO_2 levels.

MATERIALS AND METHODS

Plant Materials and Growth Conditions

The wild type was Arabidopsis (*Arabidopsis thaliana*) ecotype Columbia-0. *pifQ* (Leivar et al., 2009), hemagglutinin (HA)-tagged *PIF5ox* (Lorrain et al., 2008), *PIF5ox* (PIF5-OXL2; Fujimori et al., 2004), *max2-1* (Stirnberg et al., 2002), *yucca-D* (Zhao et al., 2001), *DR5*::*GUS* (Ulmasov et al., 1997), *pS15-5E*::*GUS* (Walcher and Nemhauser, 2012), and *DII-VENUS* (Brunoud et al., 2012) were as described previously. True-breeding lines expressing *PKS4*::*GUS* (Schepens et al., 2008) were generated from seeds of primary transformants (T1 seeds) provided by Christian Fankhauser (University of Lausanne). Seeds were sterilized (20 min in 70% ethanol, 0.01% Triton X-100, followed by a rinse in 95% ethanol), suspended in 0.1% agar (BP1423; Fisher Scientific), spotted on plates containing 0.5× Linsmaier and Skoog (LS; LSP03; Caisson Laboratories) with 0.8% phytoagar (40100072-1; Plant Media: bioWORLD), and stratified in the dark at 4°C for 3 d. For nitrogen deprivation experiments, medium was prepared from 0.5× Murashige and Skoog without nitrogenous compounds (MSP07; Caisson Laboratories) and supplemented with either 0.5 mM KNO_3 or 0.5 mM KCl. Plates were placed vertically at dawn in a Percival E-30B growth chamber set at 20°C in 60 μmol m^{-2} s^{-1} white light (unless otherwise specified) with short-day conditions (8 h of light, 16 h of dark). Controlled CO_2 chambers were as described previously (Kinmonth-Schultz and Kim, 2011). Briefly, chambers with either ambient CO_2 (approximately 400 μL L^{-1}) or elevated CO_2 (approximately 800 μL L^{-1}) were housed in the Douglas Research Conservatory (Center for Urban Horticulture, University of Washington). Seedlings were grown in two sets of paired chambers under natural light supplemented by 12 h of artificial light (high-pressure sodium 400-W single-phase bulbs; Phillips Electronics North America). Light intensity was variable across the day, with an average intensity during the light period of approximately 75 μmol m^{-2} s^{-1} and a maximum of 300 μmol m^{-2} s^{-1}. Temperature was approximately 19°C at night and 24°C during the day.

Chemical Treatments

Suc (S2; Fisher Scientific) and D-mannitol (69-65-8; Acros Organics) treatments were performed at a final concentration of 88 mM (equal to 3% [w/v] Suc). NPA (33371; Sigma-Aldrich) was suspended in dimethyl sulfoxide. Picloram (4-amino-3,5,6-trichloro-2-pyridinecarboxylic acid; P5575; Sigma-Aldrich) and IAA (705490; bioWORLD) were suspended in 80% ethanol. NPA and picloram were diluted directly into plate medium. One milliliter of 125 μM IAA (in 0.5× LS) was sprayed onto seedlings on days 3 and 4. For application of microdrops, IAA was mixed with hydrous lanolin (NCD 0168-0051-31; Fougera Pharmaceuticals) to a final concentration of 1.5 mM. A control lanolin mixture was made with an equivalent volume of solvent. These mixtures were thinned by warming to 50°C and applied to the distal portion of one cotyledon with a small wire loop. Treated seedlings were returned to growth chambers for 4.5 h before GUS staining.

Seedling Measurements and Microscopy

Time-lapse photography was as described previously (Stewart et al., 2011). Briefly, images were captured every 30 min by a CCD camera (PL-B781F; PixeLINK) equipped with a lens (NMV-25M1; Navitar) and an infrared long-pass filter (LP830-35.5; Midwest Optical Systems). Image capture was accompanied by a 0.5-s flash of infrared light by a custom-built light-emitting diode infrared illuminator (512-QED234; Mouser Electronics). A custom LabVIEW (National Instruments) program controlled image capture and illumination. For growth rate analysis from time-lapse photography, hypocotyl lengths from at least 12 individuals were measured using ImageJ software (http:/rsb.info.nih.gov/ij/) for each time-lapse image (2,208 × 3,000 pixels). Growth rates were calculated from hypocotyl lengths using a custom script in MATLAB (MathWorks), available on request. Hypocotyl or primary root lengths of 12 to 25 seedlings per condition were measured from scans of vertical plates using ImageJ software in at least two independent experiments. Plates were scanned on day 5 for plates without Suc and on day 6 for plates with Suc to match developmental stage (Stewart et al., 2011). Scans for the growth rate analysis were performed on the days indicated in Figure 1, A and B. Color seedling images were collected at 10× magnification using a Leica dissecting scope (S8APO) and camera (DFC290). Fluorescence images of root tips were captured directly from seedlings on plates using a Leica DMI 3000B microscope fitted with a Leica long-working 10× HCX PL FLUORTAR objective and illuminated with a Lumencor SOLA light source. Images were captured using Leica LAS AF version 2.6.0 software and a Leica DFC 345FX camera. Fluorescence quantification was done using ImageJ software. Mean values for 25 primary root tips per treatment were estimated using an elliptical region of interest centered on the root tip with values from root tips of untransformed plants used to subtract background fluorescence. Three biological replicates were performed with similar results.

GUS Staining

Seedlings were collected on day 5 for plates without Suc and day 6 for those with Suc and immersed in 90% acetone (v/v, with deionized water) for 20 min, washed twice with 50 mM Na_2PO_4, pH 7.2, before a 16- to 17-h incubation at 37°C in the dark with GUS reaction buffer [50 mm $NaPO_4$, 0.1% Triton X-100, 1 mm $K_4Fe(CN_6)$-$3H_2O$, 1 mm $K_3Fe(CN_6)$, and 0.5 mg mL^{-1} 5-bromo-4-chloro-3-indolyl-β-D-GlcA (Rose Scientific)]. Stained seedlings were fixed in 50% ethanol, 3.7% formaldehyde, and 5% acetic acid, and chlorophyll was removed with an ethanol series. Seedlings were rehydrated and mounted on glass slides in 40% glycerol.

Quantification of Photosynthetic Rate

Fifteen milligrams of seeds was sterilized and sown on no Suc, Suc, and mannitol media as described above. Seedling gas-exchange measurements were quantified on day 6 with an open gas-exchange system (LI-6400; Li-Cor) fitted with a specialized chamber (6400-17; Whole Plant Arabidopsis Chamber; Li-Cor) and controllable light source (6400-18; RGB Light Source; Li-Cor). Data for light-response curves were collected directly from seedlings on plates, with measurements taken at photosynthetically active radiation levels of 750, 500, 250, 120, 60, 30, and 0 μmol m^{-2} s^{-1}. Chamber air temperature was maintained at 25°C, and CO_2 reference concentration was maintained at 380 μmol CO_2 mol^{-1}. Seedling tissue was weighed at the completion of the experiment. CO_2 assimilation rates were calculated with the manufacturer's equations modified to normalize to fresh weight.

Cotyledon Area and Stomatal Density Quantification

Seedlings were grown without Suc. On day 6, seedlings were cleared with an ethanol series, fixed in 50% ethanol, 3.7% formaldehyde, and 5% acetic acid, stained with 0.5% toluidine blue O (CAS no. 92-31-9) for 4 min, and then rehydrated and mounted in 25% glycerol. Stomata were manually counted in a 0.1-mm^2 area on the adaxial side of 10 cotyledons per genotype with the ImageJ Cell Counter plugin (http://rsbweb.nih.gov/ij/plugins/cell-counter.html).

IAA Quantification

Seedlings were grown vertically on 0.5× LS plates with 2% phytoagar. Tissue was harvested from approximately 250 to 1,000 seedlings and purified as described previously with minor modifications (Andersen et al., 2008). Hypocotyls or roots were manually dissected at the time of collection. All samples were immediately frozen in liquid nitrogen and stored at −80°C or on dry ice until processing. Before extraction and purification, 1,000 or 500 pg of [$^{13}C_6$]IAA internal standard was added to each shoot or root sample, respectively. After derivatization, the samples were analyzed by gas chromatography-selected reaction monitoring-mass spectrometry (Edlund et al., 1995). Four replicates were analyzed for each sample and normalized to the fresh weight of the source tissue.

Transcriptional Analysis

Seedlings were grown vertically on 0.5× LS plates with 2% phytoagar. Expression analysis was performed on seedlings collected at dawn on day 5 for plates without

Suc and on day 6 for plates with Suc to match developmental stage. Shoots, cotyledon and hypocotyl tissue, and roots were manually dissected at the time of collection. All samples were immediately frozen in liquid nitrogen and stored at −80°C until processing. Total RNA was extracted from tissue of approximately 1,000 seedlings using the Spectrum Plant Total RNA Kit (Sigma), total RNA was treated with DNaseI on columns (Qiagen), and 2 μg of eluted RNA was used for complementary DNA synthesis using iScript (Bio-Rad). Samples were analyzed using SYBR Green Supermix (Bio-Rad) reactions run in a Chromo4 Real-Time PCR system (MJ Research). Expression for each gene was calculated using the formula (Pfaffl, 2001) $(E_{target})^{-\Delta CPtarget(control-sample)}/(E_{ref})^{-\Delta CPref(control-sample)}$ and normalized to a reference gene. Primer sequences are listed in Supplemental Table S2.

Western-Blot Analysis

PIF5-HA abundance was detected in extracts of whole *PIF5HAox* and wild-type seedlings collected at dawn on day 5. All samples were immediately frozen in liquid nitrogen and stored at −80°C until processing. Total protein was extracted from approximately 100 mg of tissue using a previously described method (Duek et al., 2004), except that anti-HA-peroxidase (Roche) was used at a 1:1,000 dilution. Anti-actin antibodies (A0480; Sigma) were used at a 1:2,000 dilution and detected with anti-mouse antibodies (172-1011; Bio-Rad) used at a 1:20,000 dilution. SuperSignal West Femto Maximum Sensitivity Substrate (Pierce) was used to detect signals. Blots shown are representative of at least two experiments with independent biological replicates.

Supplemental Data

The following materials are available in the online version of this article.

Supplemental Figure S1. Suc increases rootward staining of a reporter for an auxin-induced gene.

Supplemental Figure S2. Primary roots of *pifQ* mutant seedlings are longer than the wild type and show a reduced response to Suc.

Supplemental Figure S3. Neither Suc nor picloram has a large effect on *PIF* gene expression.

Supplemental Figure S4. Overexpression of *PIF5* results in altered cotyledon development.

Supplemental Figure S5. Effects of Suc cannot be attributed solely to osmotic stress.

Supplemental Table S1. Analysis of gene expression in response to Suc or picloram.

Supplemental Table S2. Primers used for expression analysis.

ACKNOWLEDGMENTS

We are indebted to Takato Imaizumi, Soo-Hyung Kim, Janneke Hille Ris Lambers, Elizabeth Van Volkenburgh, Hannah Kimonth-Schultz, and Britney Moss for critique of the manuscript and expert advice. We are also grateful to Andrej Arsovski and Emily Palm for providing assistance with the carbon assimilation assays and to Kylee Peterson for guidance in stomatal density assays. We thank Soo-Hyung Kim for allowing us access to his controlled CO_2 growth chambers and Ottoline Leyser, Christian Fankhauser, and Teva Vernoux for sharing seed stocks.

Received August 16, 2012; accepted October 10, 2012; published October 16, 2012.

LITERATURE CITED

Andersen SU, Buechel S, Zhao Z, Ljung K, Novák O, Busch W, Schuster C, Lohmann JU (2008) Requirement of B_2-type cyclin-dependent kinases for meristem integrity in *Arabidopsis thaliana*. Plant Cell **20:** 88–100

Bennett T, Sieberer T, Willett B, Booker J, Luschnig C, Leyser O (2006) The Arabidopsis MAX pathway controls shoot branching by regulating auxin transport. Curr Biol **16:** 553–563

Blilou I, Xu J, Wildwater M, Willemsen V, Paponov I, Friml J, Heidstra R, Aida M, Palme K, Scheres B (2005) The PIN auxin efflux facilitator network controls growth and patterning in Arabidopsis roots. Nature **433:** 39–44

Brunoud G, Wells DM, Oliva M, Larrieu A, Mirabet V, Burrow AH, Beeckman T, Kepinski S, Traas J, Bennett MJ, et al (2012) A novel sensor to map auxin response and distribution at high spatio-temporal resolution. Nature **482:** 103–106

Chapman EJ, Greenham K, Castillejo C, Sartor R, Bialy A, Sun TP, Estelle M (2012) Hypocotyl transcriptome reveals auxin regulation of growth-promoting genes through GA-dependent and -independent pathways. PLoS ONE **7:** e36210

Covington MF, Harmer SL (2007) The circadian clock regulates auxin signaling and responses in Arabidopsis. PLoS Biol **5:** e222

Dello Ioio R, Nakamura K, Moubayidin L, Perilli S, Taniguchi M, Morita MT, Aoyama T, Costantino P, Sabatini S (2008) A genetic framework for the control of cell division and differentiation in the root meristem. Science **322:** 1380–1384

Dobrenel T, Marchive C, Sormani R, Moreau M, Mozzo M, Montané MH, Menand B, Robaglia C, Meyer C (2011) Regulation of plant growth and metabolism by the TOR kinase. Biochem Soc Trans **39:** 477–481

Dowson-Day MJ, Millar AJ (1999) Circadian dysfunction causes aberrant hypocotyl elongation patterns in Arabidopsis. Plant J **17:** 63–71

Duek PD, Elmer MV, van Oosten VR, Fankhauser C (2004) The degradation of HFR1, a putative bHLH class transcription factor involved in light signaling, is regulated by phosphorylation and requires COP1. Curr Biol **14:** 2296–2301

Edlund A, Eklof S, Sundberg B, Moritz T, Sandberg G (1995) A microscale technique for gas chromatography-mass spectrometry measurements of picogram amounts of indole-3-acetic acid in plant tissues. Plant Physiol **108:** 1043–1047

Forde BG (2002) Local and long-range signaling pathways regulating plant responses to nitrate. Annu Rev Plant Biol **53:** 203–224

Franklin KA, Lee SH, Patel D, Kumar SV, Spartz AK, Gu C, Ye S, Yu P, Breen G, Cohen JD, et al (2011) Phytochrome-interacting factor 4 (PIF4) regulates auxin biosynthesis at high temperature. Proc Natl Acad Sci USA **108:** 20231–20235

Fujimori T, Yamashino T, Kato T, Mizuno T (2004) Circadian-controlled basic/helix-loop-helix factor, PIL6, implicated in light-signal transduction in Arabidopsis thaliana. Plant Cell Physiol **45:** 1078–1086

Gonzali S, Novi G, Loreti E, Paolicchi F, Poggi A, Alpi A, Perata P (2005) A turanose-insensitive mutant suggests a role for WOX5 in auxin homeostasis in Arabidopsis thaliana. Plant J **44:** 633–645

Grunewald W, Friml J (2010) The march of the PINs: developmental plasticity by dynamic polar targeting in plant cells. EMBO J **29:** 2700–2714

Hietakangas V, Cohen SM (2009) Regulation of tissue growth through nutrient sensing. Annu Rev Genet **43:** 389–410

Kiba T, Kudo T, Kojima M, Sakakibara H (2011) Hormonal control of nitrogen acquisition: roles of auxin, abscisic acid, and cytokinin. J Exp Bot **62:** 1399–1409

Kinmonth-Schultz H, Kim SH (2011) Carbon gain, allocation and storage in rhizomes in response to elevated atmospheric carbon dioxide and nutrient supply in a perennial C3 grass, Phalaris arundinacea. Funct Plant Biol **38:** 797–807

Kircher S, Schopfer P (2012) Photosynthetic sucrose acts as cotyledon-derived long-distance signal to control root growth during early seedling development in Arabidopsis. Proc Natl Acad Sci USA **109:** 11217–11221

Krouk G, Lacombe B, Bielach A, Perrine-Walker F, Malinska K, Mounier E, Hoyerova K, Tillard P, Leon S, Ljung K, et al (2010) Nitrate-regulated auxin transport by NRT1.1 defines a mechanism for nutrient sensing in plants. Dev Cell **18:** 927–937

Kumar SV, Lucyshyn D, Jaeger KE, Alós E, Alvey E, Harberd NP, Wigge PA (2012) Transcription factor PIF4 controls the thermosensory activation of flowering. Nature **484:** 242–245

Leivar P, Quail PH (2011) PIFs: pivotal components in a cellular signaling hub. Trends Plant Sci **16:** 19–28

Leivar P, Tepperman JM, Monte E, Calderon RH, Liu TL, Quail PH (2009) Definition of early transcriptional circuitry involved in light-induced reversal of PIF-imposed repression of photomorphogenesis in young *Arabidopsis* seedlings. Plant Cell **21:** 3535–3553

Li L, Ljung K, Breton G, Schmitz RJ, Pruneda-Paz J, Cowing-Zitron C, Cole BJ, Ivans LJ, Pedmale UV, Jung H-S, et al (2012) Linking photoreceptor excitation to changes in plant architecture. Genes Dev **26:** 785–790

Ljung K, Bhalerao RP, Sandberg G (2001) Sites and homeostatic control of auxin biosynthesis in Arabidopsis during vegetative growth. Plant J **28:** 465–474

Lorrain S, Allen T, Duek PD, Whitelam GC, Fankhauser C (2008) Phytochrome-mediated inhibition of shade avoidance involves degradation of growth-promoting bHLH transcription factors. Plant J **53:** 312–323

Macgregor DR, Deak KI, Ingram PA, Malamy JE (2008) Root system architecture in *Arabidopsis* grown in culture is regulated by sucrose uptake in the aerial tissues. Plant Cell **20:** 2643–2660

Moon J, Zhu L, Shen H, Huq E (2008) PIF1 directly and indirectly regulates chlorophyll biosynthesis to optimize the greening process in Arabidopsis. Proc Natl Acad Sci USA **105:** 9433–9438

Nozue K, Covington MF, Duek PD, Lorrain S, Fankhauser C, Harmer SL, Maloof JN (2007) Rhythmic growth explained by coincidence between internal and external cues. Nature **448:** 358–361

Nozue K, Harmer SL, Maloof JN (2011) Genomic analysis of circadian clock-, light-, and growth-correlated genes reveals PHYTOCHROME-INTERACTING FACTOR5 as a modulator of auxin signaling in Arabidopsis. Plant Physiol **156:** 357–372

Nozue K, Maloof JN (2006) Diurnal regulation of plant growth. Plant Cell Environ **29:** 396–408

Paul MJ, Foyer CH (2001) Sink regulation of photosynthesis. J Exp Bot **52:** 1383–1400

Pfaffl MW (2001) A new mathematical model for relative quantification in real-time RT-PCR. Nucleic Acids Res **29:** e45

Poorter H, Niklas KJ, Reich PB, Oleksyn J, Poot P, Mommer L (2012) Biomass allocation to leaves, stems and roots: meta-analyses of interspecific variation and environmental control. New Phytol **193:** 30–50

Ruffel S, Krouk G, Ristova D, Shasha D, Birnbaum KD, Coruzzi GM (2011) Nitrogen economics of root foraging: transitive closure of the nitrate-cytokinin relay and distinct systemic signaling for N supply vs. demand. Proc Natl Acad Sci USA **108:** 18524–18529

Schepens I, Boccalandro HE, Kami C, Casal JJ, Fankhauser C (2008) PHYTOCHROME KINASE SUBSTRATE4 modulates phytochrome-mediated control of hypocotyl growth orientation. Plant Physiol **147:** 661–671

Stewart JL, Maloof JN, Nemhauser JL (2011) PIF genes mediate the effect of sucrose on seedling growth dynamics. PLoS ONE **6:** e19894

Stirnberg P, van De Sande K, Leyser HM (2002) MAX1 and MAX2 control shoot lateral branching in Arabidopsis. Development **129:** 1131–1141

Stitt M, Krapp A (1999) The interaction between elevated carbon dioxide and nitrogen nutrition: the physiological and molecular background. Plant Cell Environ **22:** 583–621

Sun J, Qi L, Li Y, Chu J, Li C (2012) PIF4-mediated activation of YUCCA8 expression integrates temperature into the auxin pathway in regulating Arabidopsis hypocotyl growth. PLoS Genet **8:** e1002594

Toledo-Ortiz G, Huq E, Rodríguez-Concepción M (2010) Direct regulation of phytoene synthase gene expression and carotenoid biosynthesis by phytochrome-interacting factors. Proc Natl Acad Sci USA **107:** 11626–11631

Ulmasov T, Murfett J, Hagen G, Guilfoyle TJ (1997) Aux/IAA proteins repress expression of reporter genes containing natural and highly active synthetic auxin response elements. Plant Cell **9:** 1963–1971

Walcher CL, Nemhauser JL (2012) Bipartite promoter element required for auxin response. Plant Physiol **158:** 273–282

Walch-Liu P, Ivanov II, Filleur S, Gan Y, Remans T, Forde BG (2006) Nitrogen regulation of root branching. Ann Bot (Lond) **97:** 875–881

Zhao Y, Christensen SK, Fankhauser C, Cashman JR, Cohen JD, Weigel D, Chory J (2001) A role for flavin monooxygenase-like enzymes in auxin biosynthesis. Science **291:** 306–309